P17101: Design of a 1kW Arcjet Thruster

Philip Linden*, James Gandek†, Dylan Bruce†, Matt Giuffre†, Anthony Higgins‡, David Yin‡§

***Abstract*—An electrothermal propulsion system was developed for RIT Space Exploration (SPEX) to develop opportunities for design, testing, and characterization of advanced space systems at the Rochester Institute of Technology such as high-efficiency in-space propulsion for station-keeping maneuvers. The thruster assembly generates an electrical arc across the thruster nozzle's throat, ionizing nitrogen or argon propellant in order to achieve a greater specific impulse compared to cold gas propulsion.**

NOMENCLATURE

$\dot{m}$	Gas mass flow rate	$\mathrm{kg\,s^{-1}}$
A	Cross-sectional area of nozzle	$\mathrm{m^2}$
F	Thrust	N
g_0	Standard acceleration due to gravity	$9.81\,\mathrm{m\,s^{-2}}$
I_{sp}	Specific impulse	s
p	Gas pressure	kPa
v	Gas flow velocity	$\mathrm{m\,s^{-1}}$

I. INTRODUCTION

RIT Space Exploration (SPEX) provided a use-case scenario to serve as the basis for this exploration into satellite propulsion. The mission objective is to design a communications satellite that is capable of maintaining a polar geostationary orbit for 10 years.

In practice, satellites in Earth orbit for long-duration missions (5–25 years) encounter perturbations to their trajectories over time from residual atmospheric and orbital particles, or from variations in Earth's gravity field. These spacecraft perform short station-keeping maneuvers periodically to compensate for drift and orbital decay.

An electrothermal rocket engine is method of propulsion by which a pressurized inert gas stored at ambient temperature (cold gas) is released and heated electrically before being expelled out of a nozzle. Two proven methods of electrothermal propulsion are *resistojets*, which use conventional heat exchangers to heat the propellant, and *arcjets*, which pass the propellant through an electrical arc to heat the gas.

Electrothermal propulsion is advantageous over conventional chemical or cold-gas rockets for use by long-life satellites since the engines may be small in size, have no moving parts, and are more efficient at the expense of thrust. While resistojets and arcjets require more elecrical power than chemical rockets, for example, the electrical energy may be recovered over time by photovoltaic panels whereas propellant fuel is a finite resource for these spacecraft.

A tabletop prototype thruster was designed and tested to explore the feasibility of this type of system with less strict requirements compared to the limitations of building a flight-worthy system. A tabletop version does not require integration with a spacecraft, and mass and spatial limitations are relaxed.

II. DESIGN THEORY

In low power ($1\,\mathrm{kW}$) applications, an arcjet offers up to 200% gains in efficiency over a resistojet thruster [1]. Figure 1 identifies the typical use cases and performance characteristics of arcjets compared to various other types of electrothermal thrusters. Arcjets achieve a greater specific impulse compared to resistojets but produce less thrust. Thus a maneuver would take a longer amount of time using an arcjet but would consume less propellant overall for the same maneuver as compared to a resistojet.

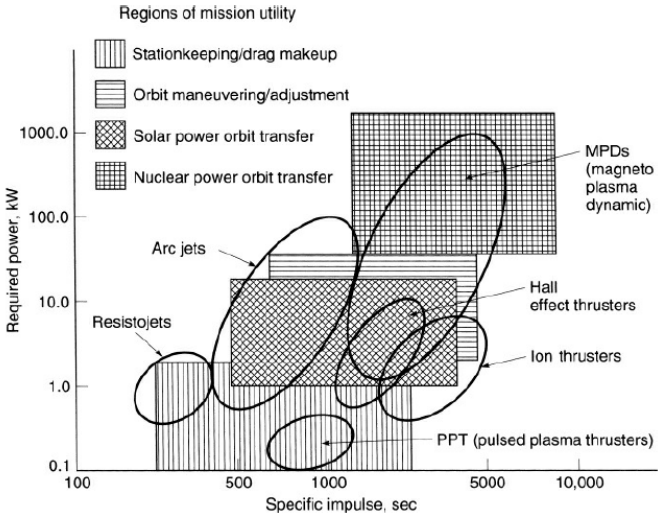

Fig. 1. There are various types of electrothermal propulsion with respect to typical performance and mission utility. In the $1\,\mathrm{kW}$ range, arcjets typically have a higher specific impulse than resistojets. (Sutton 2010)

The ideal propellant for arcjet engines is one which can be stored for long periods of time, has a low atomic mass, and favorable thermodynamic conditions during heating and expansion. NASA identifies Hydrogen (H_2), Ammonia (NH_3), and Hydrazine (N_2H_3) as ideal propellants for arcjets [2]. Unfortunately, these gases are toxic or difficult to handle on a university campus. Nitrogen (N_2) is an easy-to-handle alternative that has relatively favorable ionization and thermodynamic characteristics, and has been used in similar low-power arcjet demonstrations [3], [4]. Argon (Ar) is a very cheap, easy-to-handle, and highly available alternative to nitrogen, and has similar characteristics.

*MEng Student, Department of Mechanical Engineering
†BS Student, Department of Mechanical Engineering
‡BS Student, Department of Electrical Engineering
§Only contributed to MSD I

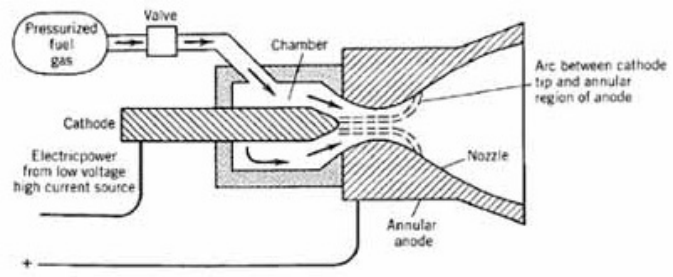

Fig. 2. A cross sectional view of a typical arcjet shows the expected flowpath of propellant and the expected region of the electric current arc. The propellant is ionized and heated by the arc then expanded through the nozzle. (NASA GRC 1992)

Gas enters the chamber and is ionized and heated by a high-current arc that extends from the cathode to the throat of the anodic nozzle to form a plasma. The plasma reaches sonic speed in the throat and is supersonically accelerated as it expands through the nozzle. Ideal flow performance is illustrated in Figure 3, assuming uniform flow across nozzle cross sections, isentropic flow conditions (except across shocks), zero vorticity, and unmoving flow at inlet.

Thrust is a function of the momentum of the flow exiting the nozzle.

$$F = \dot{m}v_e + (p_e - p_b)A_e \tag{1}$$

Where F is thrust, $\dot{m}$ is mass flow rate of propellant, v is flow velocity, A is nozzle cross sectional area of the nozzle, and subscript e denotes parameters at the nozzle exit while p_b denotes atmospheric backpressure. In space, p_b is negligible and the thruster is design around such condition.

A thruster's efficiency is described in terms of specific impulse, I_{sp}, which may be used to compare performance with other space propulsion methods.

$$I_{sp} = \frac{F}{\dot{m}g_0} \tag{2}$$

In the ideal condition using gaseous N_2 as propellant, a conical nozzle with $\alpha = 15$ is capable of 0 N of thrust without a sustained arc. At sea-level, 0 N of thrust is expected. Include theoretical calcs for cold thrust to compare performance with theory in order to validate design. Show I_{sp} predictions for given thrust values and estimated mass flow rates.

TABLE I. THEORETICAL THRUST AND I_{sp} VALUES WITH RESPECT TO SPACE AND SEA-LEVEL OPERATION, TOTAL PRESSURE p_0 =239.2 kPa.

		Without arc		With arc	
	p_b (kPa)	Thrust (N)	I_{sp} (s)	Thrust (N)	I_{sp} (s)
Vacuum	0	0	0	0	0
Sea-level	101.3	0	0	0	0

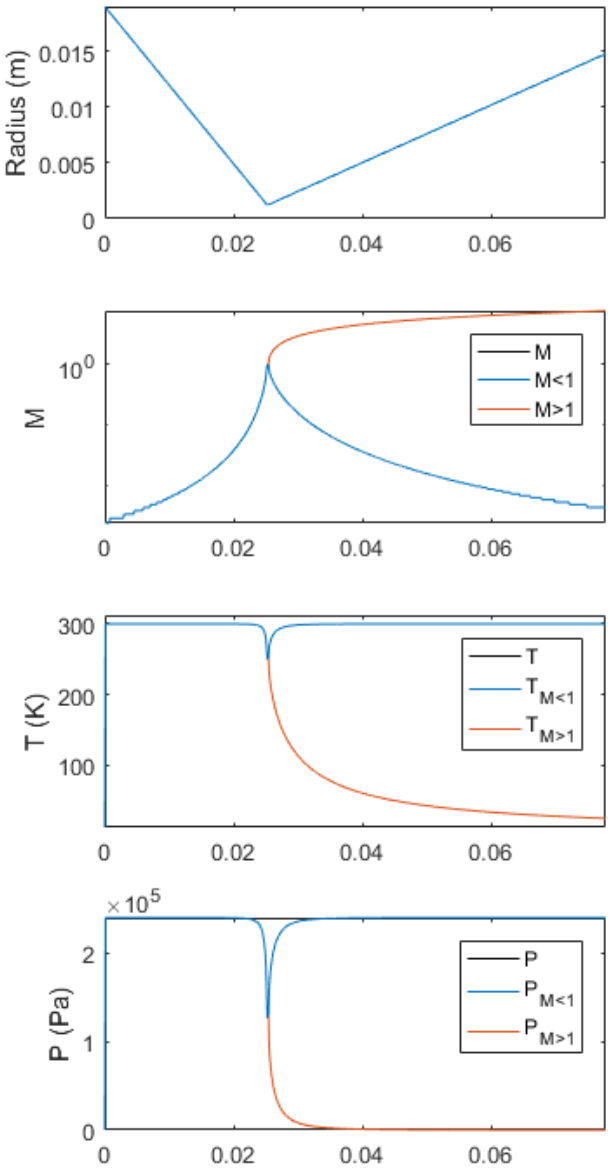

Fig. 3. Update with predicted flow through nozzle, including shocks.

III. System Overview

A. Thruster

Propellant flows into a stainless steel body and is spun into a vortex about the tip of the cathode, where it passes through an

electric arc before being accelerated through a conical nozzle. The flow swirler doubles as a high-temperature ceramic insulator. The insulator and cathode are mounted concentrically into a low-temperature PTFE thermal and electrical insulator, which is fixed to the thruster test stand. The nozzle is electrically insulated from the steel body by a non-conductive ceramic spacer.

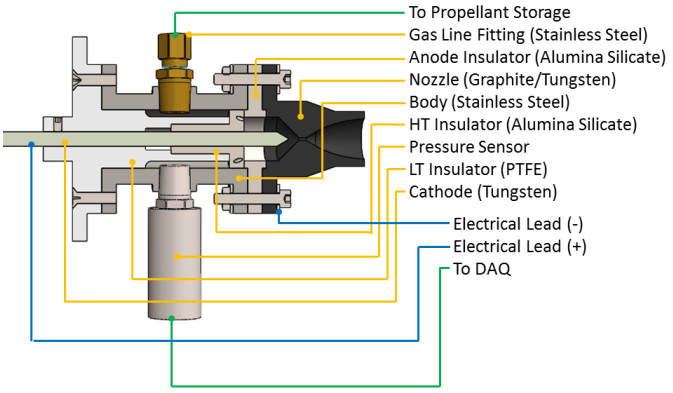

Fig. 4. Components that are charged or exposed to extreme heat are electrically and thermally insulated. Update with HV+ lead and remove tungsten material from nozzle.

B. Power Conditioning Unit

The electrical arc used to add energy to the gas is generated and sustained by the Power Conditioning Unit (PCU). The PCU consists of separate high-voltage (HV) and high-current (HC) sides. The HV side of the circuit initiates the arc, then the PCU switches to the HC "side" of the circuit to sustain a high-current arc. This architecture is similar to a plasma torch and has been demonstrated in similar tabletop systems [5].

120 V AC power is supplied to the PCU from a standard wall outlet. The HV side of the circuit raises the voltage by several orders of magnitude. A tungsten rod serves as the cathode of the HV circuit, and the graphite nozzle of the thruster acts as the anode. When the arc jumps between the cathode and anode across the flowpath, it closes the HC portion of the circuit. This current passes through a coil that activates a reed switch, turning off the HV side of the PCU.

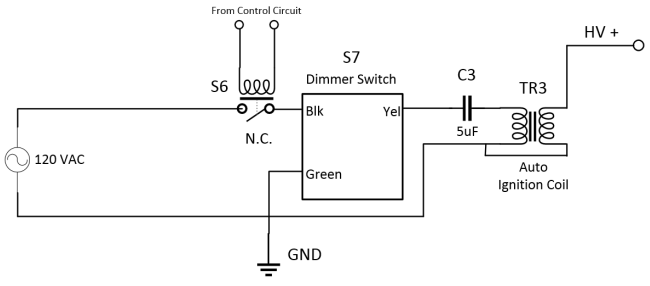

Fig. 5. Wall AC power is converted to DC high voltage in order to initiate an arc.

The control circuit for the high current works by utilizing a lower voltage DC source. To achieve this, the 120 V AC signal is passed through a step down transformer and is rectified to DC. A normally open reed switch is used to detect current passing through the coil in the HC circuit. When closed, the DC voltage is applied to the relay in the HV circuit. The relay is normally closed, so applying a voltage to it disables the HV side.

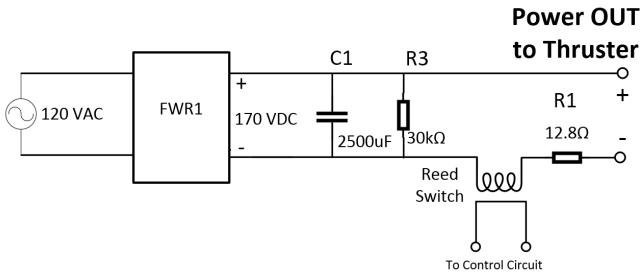

Fig. 6. A schematic of the components used in the HC circuit. The 120V AC line from the wall gets rectified into a DC voltage with a power resistor controlling the current draw.

The HC circuit works by rectifying the 120 V AC sine wave, resulting 170 V DC. The arc closes the circuit, allowing electrons to flow. The high current is drawn from heating coils acting as power resistors. The two heating coils can be configured to have a resistance of 7.5 Ω, 15 Ω, or 30 Ω. All tests were performed with the 15 Ω configuration. The HC circuit has a coil that activates a reed switch when on. The reed switch activates a relay which turns off the HV circuit.

The PCU is housed in a modified mid-tower aluminum computer case shown in Figure 8. This provides a grounded area with many tie-down points for electrical components to be placed. The computer case is laid on its side with one side panel removed. Clearance holes for component stakes are drilled through the panels and components are secured with screws or cable ties. Two desktop computer case fans are mounted in the back of the PCU housing to provide some airflow to cool the power resistors during operation.

During nominal operation, the PCU draws 900–1100W from the wall outlet.

C. Test Stand

The test stand, shown in Figure 7, is cantilevered in design, leveraging both the mass of the thruster and its operating thrust. Because expected thrust output is less than 50 mN and load cells in this range are either very costly or lack the necessary accuracy, the thruster mass is used as an offset that suits a more common range load cell. The resolution of a 0–6kg Omega LCAE-6kg load cell was chosen as a reasonable middle ground between load resolution and cost.

The construction of the stand is largely 6061-T6 aluminum with the test platform assembled to an oil-impregnated bronze rod that allows for displacement vertically downwards on the load cell. Two 6"×8" plates are welded at a right angle with

a pair of gussets to form the main structure of the stand, and two bearing blocks are fastened several inches further up to capture the bronze bearing rod and test platform itself. The thruster is mounted to the test platform using a set of three toe-clamps to make the set up and breakdown of the system simple and efficient. The stand's construction allows for some variability in expected test results through a set of slots used to position the load cell. Since it offers a small form facto, the complete mechanical system can be accommodated in a range of different testing environments such as the engine test cell that is used to complete these initial studies.

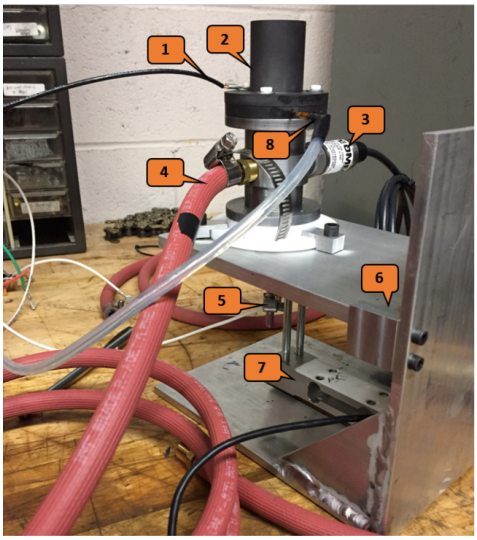

1. Nozzle Ground
2. Thruster
3. Pressure Transducer
4. Gas Inlet
5. High Current Tungsten
6. Test Stand
7. Load Cell
8. HV Tungsten

Fig. 7. An annotated view of the thruster assembly and test stand in the test configuration. *Not shown:* A compressed gas dewar with an inline flow meter and regulator valve are connected to the gas inlet tube (4) prior to the solenoid valve.

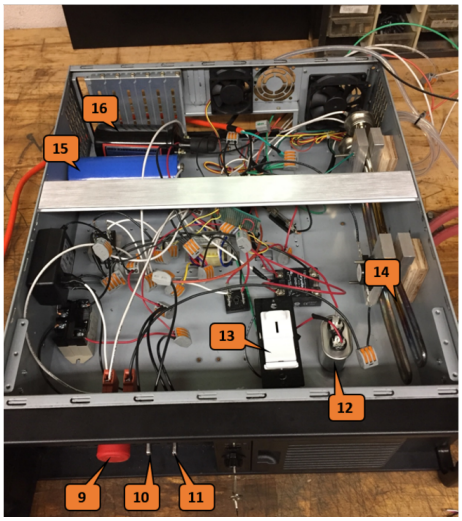

9. E-stop
10. Solenoid Control
11. PCU Control
12. HV Capacitor
13. Dimmer Switch
14. Power Resistors
15. High Current Capacitor
16. Ignition Coil

Fig. 8. An annotated view of the open PCU. Small components such as relays are not labeled here for clarity. The the top cover of the PCU housing (not shown) may be installed to enclose the system completely.

Propellant is supplied by a compressed gas dewar at 2200 psi. The GN_2 is nominally regulated to 20 psi before reaching a normally-closed solenoid valve. GN_2 is flowed through the system for several seconds before PCU ignition to ensure only propellant is present in the thruster, and after PCU shutdown to cool hot thruster components.

The propellant solenoid and PCU are activated and deactivated toggle switches next to an emergency shut-off button, shown in Figure 8.

D. Data Acquisition & Control

Data acquisition (DAQ) is collected by a National Instruments MyDAQ device utilizing a LabVIEW Virtual Interface (VI). Two DAQ devices were recognized as being readily available, the NI USB-6008 and the NI MyDAQ. The USB-6008 device offers more overall channels (4 analog input) but with a much lower throughput (10 kS/s) and resolution (12-bit). The MyDAQ device only offers 2 analog input channels but offers 200 kS/s at 16-bit resolution. It was determined that the primary performance metric would be the thrust force generated during a burn with pressure inside the main body being a secondary performance metric. Acquiring data for these metrics would only require two analog input channels and as such, the MyDAQ device was chosen for its superior precision. Both devices were also capable of generating an output which would be sufficient to actuate the transistors, which in turn activate the PCU and propellant solenoid, so this parameter was not taken into consideration during device selection. Initially the DAQ was configured to send control commands to activate and deactivate the PCU and solenoid, but was later removed due to errors encountered during testing.

The test engineer starts and stops recording a test data set with the VI (see Figure B.1) from a computer connected to the test stand. Once the proper channels are selected for data acquisition (analog inputs), the DAQ parameters may be chosen (i.e. sample rate & number of samples per channel). The test engineer may also choose whether to save test data. After a data set is collected, it is displayed on an amplitude versus time plot.

E. Safety Measures

In the event of a computer malfunction, an emergency shutoff button is wired into the circuit between the outlet and the PCU and the solenoid is normally closed and non-latching. This emergency shut-off and the toggle switches used to engage the PCU and solenoid are mounted behind a locking door such that the emergency shut-off button is pressed when the door is closed. The safety door is closed whenever the system is not in use, and locked when the system is stored.

When a test is conducted, the test stand is placed in a well-ventilated Formula SAE engine test cell, and the control computer is located outside the testing room. The VI monitors sensor data in real-time and shuts down operation when sensor parameters reach unsafe limits, and may be stopped via the stop button on the front panel or by the satisfaction of a number of safety interlocks present within the block diagram. Examples of these interlocks are errors in the DAQ sequence,

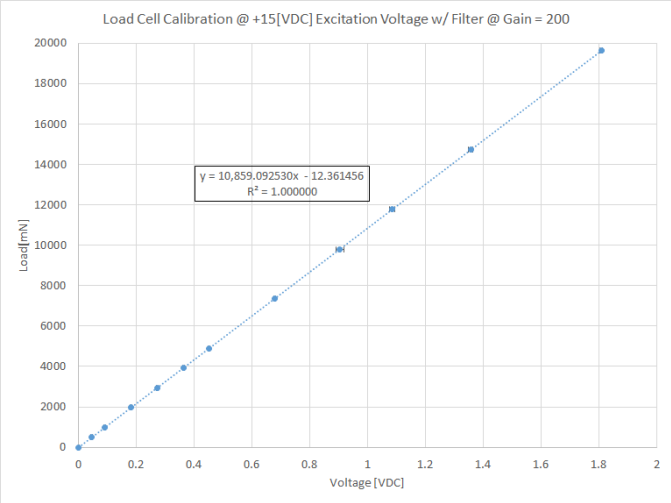

Fig. 9. Using multiple data sets for a range of known precision mass loads, output voltages from the load cell are averaged and a calibration curve is drawn. REPLACE WITH NEW CAL

positive gauge pressure present in the thruster's main body before starting the VI, or a ten second timeout.

IV. Test Procedure

The test stand, PCU, and propellant supply canister are placed in an engine test cell used by RIT's Formula SAE club. This space is typically used for engine testing and is outfitted with reinforced doors, walls, and windows, a ventilation system, and an adjacent room fitted with computers. The arcjet thruster assembly is in view of the computer room windows. Wires for data acquisition and control are fed through a pass-through between the two rooms and connected to a National Instruments myDAQ, which is connected to a computer running the DAQ VI.

The thrust load cell is calibrated in the test configuration by placing precision masses on the nozzle and recording at least 2 data sets for each calibration load. The calibration loads are used to correlate output voltage from the load cell into force data. Figure 9 shows the load cell calibration curve.

For each test, the test cell is evacuated and its doors are closed. The propellant solenoid valve opens one to two seconds before the PCU engages to purge air from the system to ensure only propellant is present in the thruster. The PCU ignites the arc and sustains it for at least five seconds. The PCU disengages and cold gas continues to flow for an additional two to five seconds in order to cool the thruster. The solenoid valve closes and the system is safed before the test cell is opened. Thrust and pressure data are saved to a comma-delimited text file.

Load cell data was collected for no operation, cold gas only, and gas flow with the PCU engaged. The data set for no operation is used to tare the thrust scale and allow the weight of the system to be filtered out of other test data sets. By collecting thrust data for cold gas only and with the PCU engaged, the effects of adding heat to the gas with an electric arc may be assessed. For each data set, volumetric flow rate was measured by a flow meter in-line and downstream from the propellant supply pressure regulator.

Fig. 10. Videos were recorded during test fires. *Far left:* The system before a test. *Center left:* The arc is generated and the propellant is partially ionized. *Center right:* A fully realized plume of plasma is sustained in the nozzle. *Far right:* After 5–10 seconds of thrust, the PCU is deactivated and the tungsten electrode glows red hot while the graphite nozzle is warm to the touch.

TABLE II. Best estimate of empirical thrust for operation in atmosphere.

Propellant	Thrust (mN)* Without arc	With arc
Nitrogen	Inconclusive	Inconclusive
Argon	4.0–10.5	7.3–14.2

* Thrust data is the average tare load (0 N) substracted from the average load observed during test fires for each propellant, after filtering.

V. Results

The PCU consistently generates and sustains an electric arc that spans from the tungsten electrode to the graphite nozzle. Using argon or nitrogen propellant, the gas is ionized and hot plasma is ejected from the nozzle, as shown in Figure 10.

Outputs from the load cell are noisy, but oscillate symmetrically about values to a precision of $\pm 10\%$ in accordance with the manufacturer specification. citation? On the millinewton scale, load cell measurement data is very noisy, and signal noise worsens while the PCU is engaged. Empirically, the true thrust load is lost in measurement error. Additional measurement error is suspected to be caused by electromagnetic interference from the high-voltage components operating in close proximity to telemetry cables.

Metrics on the true performance of the thruster is inconclusive. Reporting thrust and specific impulse from these data would be highly uncertain and misleading. However, the data shows that thrust for tests with and without the PCU engaged are significantly statistically different. While the true performance can not be quantitatively determined, it is clear that the qualitative goal of achieving a change in performance over gold gas propulsion by ionizing propellant with an electric arc has been met.

VI. Conclusions & Recommendations

Acknowledgments

The team thanks Mr. Vincent Burolla for his unwavering support; the Mechanical Engineering Department, the Multidisciplinary Senior Design Department, and the Kate Gleason College of Engineering for their resources and workspaces; RIT Space Exploration and Boeing for sponsoring this project.

REFERENCES

[1] G. Sutton and O. Biblarz, *Rocket Propulsion Elements*. Hoboken, N.J: Wiley, 2010.

[2] "Arcjet thruster design considerations for satellites," NASA GRC, Tech. Rep., 1992, https://llis.nasa.gov/lesson/736.

[3] M. Heyns, "2.2 kW nitrogen low power arcjet thruster," Master's thesis, Olin College, 2012, http://www.michaelheyns.com/index.php/projects/arcjet-thruster.

[4] M. Heyns and E. Poindexter, "Arcjet thermodynamic simulation along thruster axis," Olin College, Tech. Rep., 2012.

[5] C. Park, "Feasibility of low energy plasma torch for reaction control thruster ignition," Master's thesis, California State University, Long Beach, May 2015.

APPENDIX A
PCU SCHEMATIC

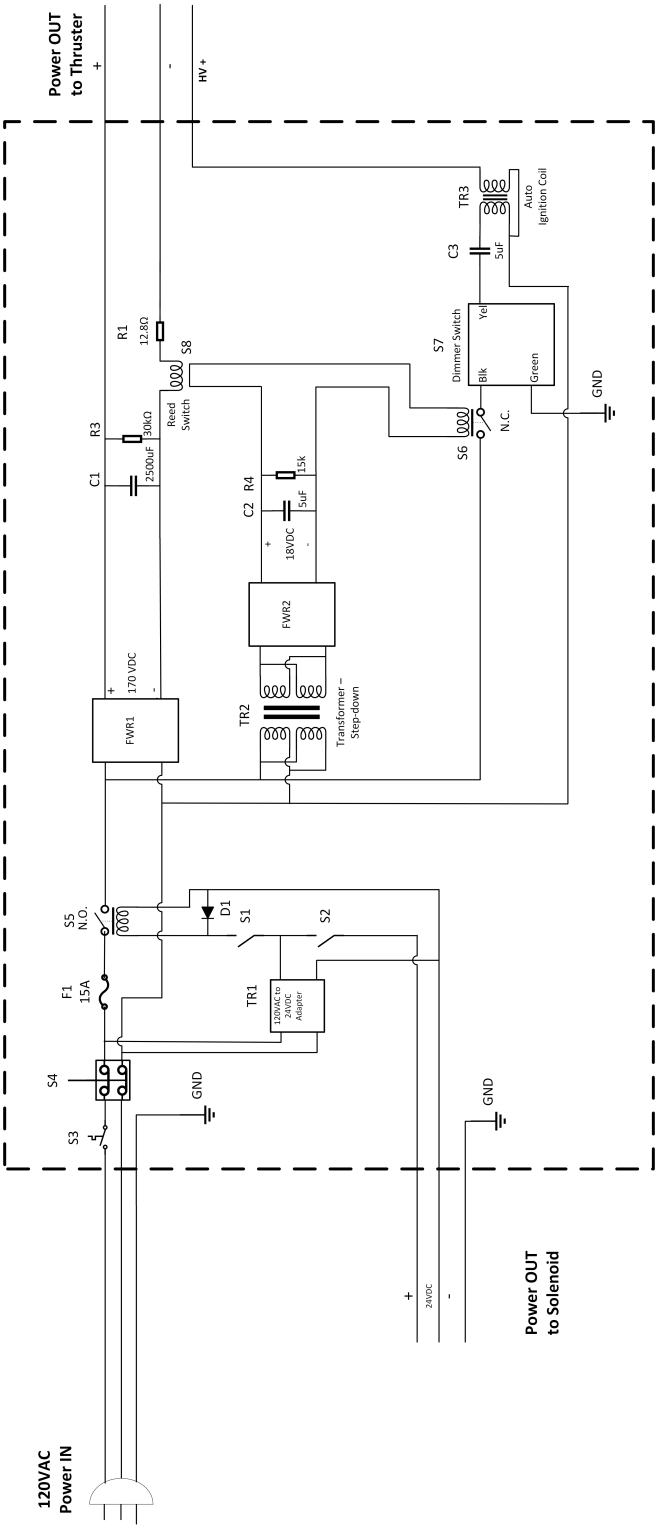

Fig. A.1. Electrical diagram of the PCU.

APPENDIX B
DATA AQCUISITION & CONTROL VIRTUAL INTERFACE

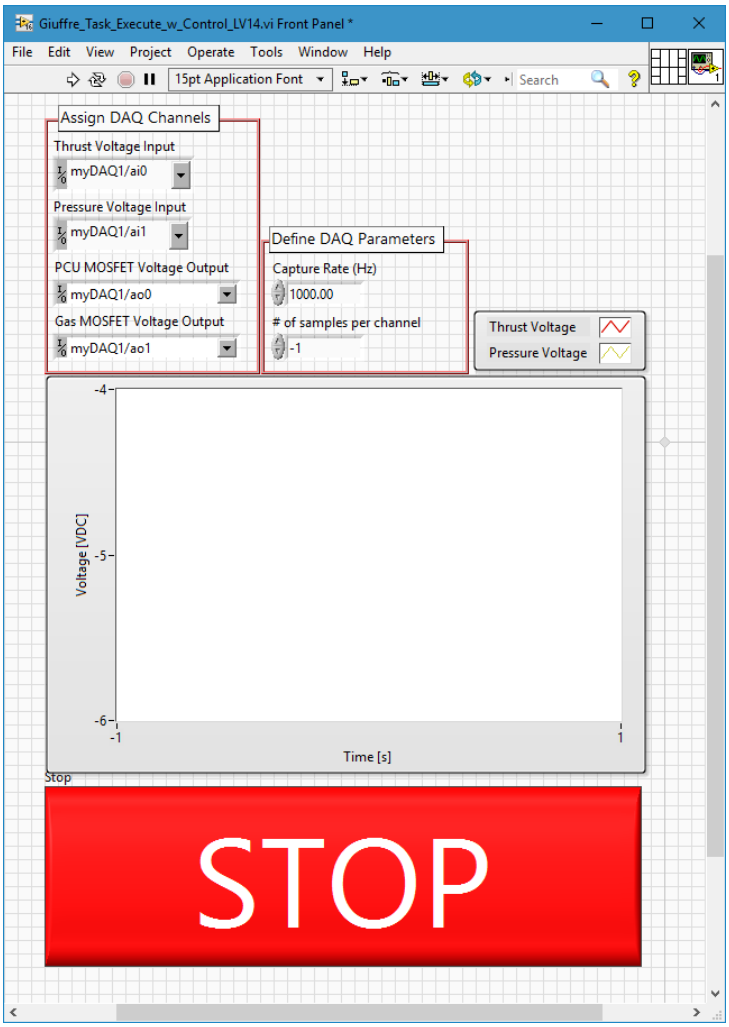

Fig. B.1. The user interface for the DAQ/Control VI.